CRYSTAL GROWTH & DESIGN

ARTICLE

pubs.acs.org/crystal

Density and Stability Differences Between Enantiopure and Racemic Salts: Construction and Structural Analysis of a Systematic Series of Crystalline Salt Forms of Methylephedrine

Alan R. Kennedy,*[,†] Catriona A. Morrison,*[,†] Naomi E. B. Briggs,[†] and William Arbuckle[‡]

[†]WestCHEM, Department of Pure and Applied Chemistry, University of Strathclyde, Glasgow G1 1XL, Scotland

[‡]MSD, Newhouse, Motherwell, Lanarkshire ML1 5SH, Scotland

Supporting Information

ABSTRACT: A data set of systematically related solid-state structures of pharmaceutical relevance has been created and used to investigate structural impact on physical properties in 20 pairs of enantiopure and racemic methylephedrinium salts. The structures are described and compared through graph-set analysis and the crystal packing similarity features of Mercury CSD 2.3. The commonest graph-set motif, $C_2^2(9)$, was found to be present in 22 of the 37 independent structures and was flexible enough to include both carboxylate and sulfonate functionalities. An equivalent $C_2^1(7)$ motif was present in all six halide structures investigated. Analysis of molecular structure found three common methylephedrinium cation conformations, while analysis of cation packing found six isostructural groups, each containing at least two salt structures and based on one of three common cation packing motifs. Melting points and crystallographically obtained densities were examined in detail for the 13 enantiopure and racemic structural pairs found to be chemically identical to each other. While average densities conform to Wallach's rule, 6 of the 13 individual pairings do not. This does not support the structural justification normally given for Wallach's rule. One of the three observed common cation packing motifs is highly associated with failure of Wallach's rule, as are significant differences in hydrogen bonding between the enantiopure and racemic structures.

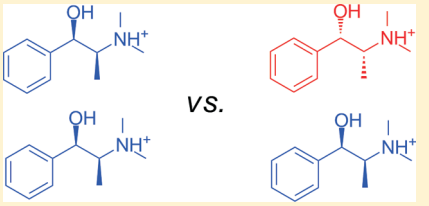

INTRODUCTION

Pharmaceutical salt formation is one of the easiest and most cost-effective ways to optimize and manipulate the material properties of a new drug[1] without altering the desired active pharmaceutical ingredients (API).[2] Salts of molecules with chiral centers are highly relevant as more than half of all patented drugs are chiral;[3] however, these are often marketed as racemates as this is the form initially produced during preparation in achiral environments.[4] Much attention has of course been paid to the characterization of enantiopure drugs in comparison to the racemic drug, due to the well-known different pharmacological effects of the two drug forms. Perhaps less well-known to the general chemistry community is that chirality affects the bulk physical properties (for instance, solubility, dissolution rate, and melting point) as well as the biological mechanisms of drug molecules.[5]

Kitaigorodskii's "principle of close packing" states that close packing ultimately equates to thermodynamic stability and that therefore the densest material will be the most thermodynamically stable.[6] Together with optimizing hydrogen-bonding and other directional intermolecular interactions, the need for packing efficiency is often taken as the driving force behind crystal formation. Wallach's rule states that racemic crystals are denser than their chiral counterparts.[7] Taking Kitaigoroskii and Wallach together gives the notion that "racemic compounds have lower enthalpies than (*their equivalent*) pure enantiomers".[8] The structural rationalization behind Wallach's rule is that array structure is different for enantiopure and racemic versions of compounds due to variation in their packing ability. Racemic compounds can crystallize in any of the 230 space groups, whereas enantiopure compounds are limited to crystallizing in only 65 chiral space groups.[9] In theory, as enantiopure crystals are only allowed to use proper symmetry operators (i.e., rotations and translations), they are unable to be as tightly packed as their equivalent racemic crystals (that can also use improper symmetry operators) and this results in a less dense compound. A higher level discussion of the structural consequences of symmetry type is given by Brock and Dunitz.[10]

Experimental evidence for Wallach's rule has always been somewhat patchy. Jacques et al.[4] compiled early work, including that of Wallach himself, and showed that the racemic form was more dense than the enantiopure in only half of the cases cited. A more complete (129 pairs of structures) and modern compilation of literature data by Brock et al.[9] did find evidence that racemic crystals are systematically slightly more dense (and have greater thermodynamic stability) than enantiopure forms. However, they also point out that their data set is inherently biased due to the differing chiral purities of the compounds used to

Received: January 10, 2011
Revised: February 8, 2011
Published: March 09, 2011

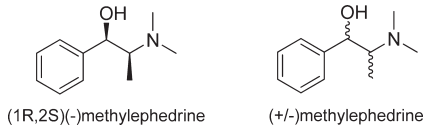

Figure 1. Enantiopure and racemic methylephedrine.

obtain the original samples. In all cases, close examination of the individual racemic and enantiopure pairs shows Wallach's rule to be false on many occasions.

With respect to pharmaceutically relevant salts, some notable experimental and theoretical studies have been carried out on enantiopure and racemic salt pairs, looking at differences in packing arrangements and lattice energies.[11] Hampering further understanding is the lack of relatively large data sets of systematically related salt structures. This is true of general salt forms of pharmaceutical or pharmaceutical-like molecules (a notable, and here highly relevant, exception to this is the work by Davy et al.)[12] and is even more apparent where pairs of enantiopure and racemic structures are required. This paper contributes data to the debate by reporting structures for 20 enantiopure and racemic salt pairs of methylephedrine, Figure 1, and by analyzing the observed differences in their crystal structures and packing.

Methylephedrine is a member of the phenylethylamine structural family, of which there are many members that have pharmaceutical significance, for example, the anti-asthma drug salbutamol, the decongestant ephedrine, and the stimulant methamphetamine. There are few known literature structural studies of methylephedrine. The structure of the enantiopure free base is deposited in the Cambridge Crystallographic Data Centre (CCDC), reference UCAWOL.[13] A structure for racemic methylephedrine has not been achieved, and indeed in our hands recrystallization of the racemic compound gave a conglomerate. The only other related work present in the CCDC is the 1934 study by Gossner, which investigated the halide salts.[14] Because of the early year of these data collections, the work does not report any atomic coordinates and therefore the structures are redetermined herein.

Twenty pairs of salt structures were obtained from enantiopure, (1*R*,2*S*)(−), and racemic, (±), methylephedrine with 20 pharmaceutically relevant counterions. The molecular structures of the 20 counterions are shown in Figure 2. This choice allows for direct comparison between the enantiopure and racemic pairs as all salts were synthesized by the same technique and crystals were grown under broadly similar conditions. Analysis of the hydrogen bonding and the crystal packing will be presented to determine similarities between structures. Their crystallographically measured densities will be examined to allow Wallach's rule to be tested and finally the experimental melting points will be inspected.

EXPERIMENTAL SECTION

Materials. All experiments were carried out using commercially available materials, apart from (±)-methylephedrine, which was formed from a 50:50 mixture of the commercially available (1*R*,2*S*)(−) and (1*S*,2*R*)(+) methylephedrine bases.

Salt Synthesis and Crystallization. All salts were prepared by the same method. This involved the reaction of a partially dissolved aqueous solution of the free base with a 10% excess equivalent of the appropriate acid in aqueous solution to form a solution of the salt. The solution was stirred for 30 min with gentle heating to 50 °C. Finally, the

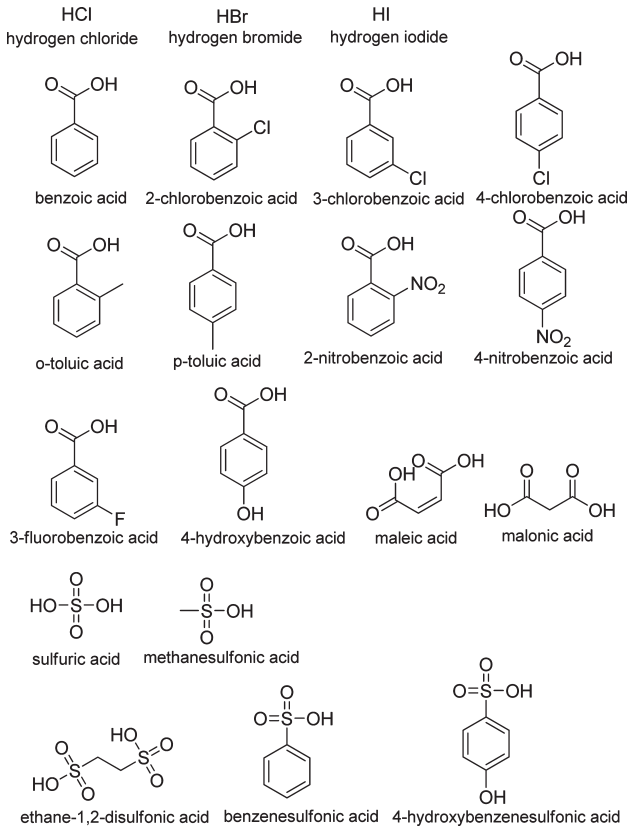

Figure 2. Molecular structures of the 20 acids used in salt formation.

solution was filtered and left to produce crystals by slow evaporation and cooling. Where unsatisfactory single crystals were recovered, these were redissolved and the resultant solution was filtered into a tube of approximate diameter 5 mm, to allow for slower evaporation and crystal growth.

Crystallographic Data Collection and Processing. Samples for single crystal diffraction studies were obtained as above. Measurements were recorded at low temperature by Bruker-Nonius CCD and Oxford Diffraction diffractometers with Mo Kα radiation (λ = 0.7107 Å) or Cu Kα radiation (λ = 1.5418 Å). Refinement of atomic coordinates and thermal parameters was to convergence and by full-matrix least-squares methods on F^2 within SHELX-97.[15] Where heavy atoms were present (S, Cl, Br, I) refinement of Flack parameters determined absolute structure. Selected crystallographic data and refinement parameters are given in Tables 1, 2 and 3 and full details are deposited as cif files. These can be obtained free of charge from The Cambridge Crystallographic Data Centre via www.ccdc.cam.ac.uk/data_request/cif by quoting deposition numbers CCDC 806488−806524.

Melting Point Determination. Melting points were collected in triplicate using a Buchi B-545 automatic melting point apparatus.

RESULTS AND DISCUSSION

For this work, salt synthesis was attempted with both the enantiopure and racemic forms of the base methylephedrine and 38 acids. In 20 cases crystals of both forms were achieved, resulting in the possibility of directly comparing the structural effect of using enantiopure versus racemic bases. Of the 20 pairs of structures, 13 are enantiopure/racemic pairs with chemically identical formula. The remaining seven pairs consist of four which are chemically different (mostly due to differing hydration states, but for salts P1 and P2 through formation of tri-iodide

Table 1. Summary of Crystallographic Data for the 13 Chemically Identical Salt Pairs

(1*R*,2*S*)(−)-methylephedrinium salts						(±)-methylephedrinium salts					
salt form	chemical formula, MW	space group	cell parameters (Å, °, Å^3), Z	R_{int}, N_{ref}, NV	R_1, wR_2, S	salt form	chemical formula, MW	space group	cell parameters (Å, °, Å^3), Z	R_{int}, N_{ref}, NV	R_1, wR_2, S
A1 2-chlorobenzoate	$C_{11}H_{18}NO$, $C_7H_4ClO_2$ 335.82	$P2_1$	a = 6.1475(5), b = 13.1347(10), c = 10.5981(9), β = 99.160(8), 844.85(12), 2	0.0352, 2584, 212	0.0459, 0.1115, 1.131	**A2** 2-chlorobenzoate	$C_{11}H_{18}NO$, $C_7H_4ClO_2$ 335.82	$Pca2_1$	a = 10.4182(6), b = 8.0374(4), c = 20.2501(14), 1695.65(17), 4	0.0358, 2891, 220	0.0396, 0.0669, 0.895
B1 2-nitrobenzoate monohydrate	$C_7H_4NO_4$, $C_{11}H_{18}NO$, H_2O 364.39	$P2_1$	a = 5.8119(2), b = 13.1776(3), c = 12.0410(4), β = 103.222(3) 897.74(5), 2	0.0132, 3271, 252	0.0259, 0.0584, 0.978	**B2** 2-nitrobenzoate monohydrate	$C_{11}H_{18}NO_4$, C_7H_4NO, H_2O 364.39	$Pbca$	a = 15.6457(3), b = 11.2144(2), c = 21.0605(4), 3695.21(12), 8	0.0237, 4039, 252	0.0334, 0.0774, 0.917
C1 3-fluorobenzoate	$C_{11}H_{18}NO$, $C_7H_4FO_2$ 319.37	$P2_1$	a = 5.8318(5), b = 13.0114(7), c = 10.8982(8), β = 97.971(4), 818.96(10), 2	0.1213, 1948, 220	0.0580, 0.1347, 1.022	**C2** 3-fluorobenzoate	$C_{11}H_{18}NO$, $C_7H_4FO_2$ 319.37	$C2/c$	a = 24.2192(13), b = 5.7476 (3), c = 23.7497(14), β = 96.799(6), 3282.8(3), 8	0.0249, 3464, 219	0.0412, 0.0962, 0.880
D1 4-nitrobenzoate	$C_{11}H_{18}NO$, $C_7H_4NO_4$ 346.38	$P2_1$	a = 5.8311(2), b = 12.9695(4), c = 23.5520(9), β = 94.839(3), 1774.81, 4	0.0356, 7760, 473	0.0373, 0.0625, 0.908	**D2** 4-nitrobenzoate	$C_{11}H_{18}NO$, $C_7H_4NO_4$ 346.38	$P2_1/c$	a = 5.8279(7), b = 12.8112(11), c = 23.317(3), β = 91.683(13), 1739.4(3), 4	0.0711, 3790, 237	0.0551, 0.1541, 0.967
E1 *o*-toluate	$C_{11}H_{18}NO$, $C_8H_7O_2$ 315.40	$P2$	a = 5.9395(8), b = 15.0195(13), c = 9.6909(13), β = 97.506(12), 857.07(18), 2	0.0623, 1566, 213	0.0319, 0.0505, 0.779	**E2** *o*-toluate	$C_{11}H_{18}NO$, $C_8H_7O_2$ 315.40	$Pca2_1$	a = 10.4716(2), b = 8.0447(2), c = 20.2936(4), 1709.55(6), 4	0.0369, 3330, 221	0.0300, 0.0711, 1.057
F1 benzenesulfonate	$C_{11}H_{18}NO$, $C_6H_5O_3S$ 337.42	$P2_1$	a = 7.4230(2), b = 11.2355(3), c = 10.5683(2), β = 93.590(2), 879.68(4), 2	0.0430, 4182, 219	0.0382, 0.0659, 0.924	**F2** benzenesulfonate	$C_{11}H_{18}NO$, $C_6H_5O_3S$ 337.42	$P2_1/c$	a = 10.4282(2), b = 10.8429(1), c = 14.9671(2), β = 94.6010(10), 1686.91(4), 4	0.0187, 3869, 219	0.0307, 0.0917, 1.109
G1 1,2-ethanedisulfonate	$C_{11}H_{18}NO$, $0.5C_2H_4O_6S_2$ 274.35	$P2_1$	a = 5.9219(12) b = 32.974(5) c = 7.1591(12) β = 99.465(2), 1378.9(4), 4	0.0194, 6108, 335	0.0353, 0.0804, 1.199	**G2** 1,2-ethanedisulfonate	$C_{11}H_{18}NO$, $0.5C_2H_4O_6S_2$ 274.35	$P2_1/c$	a = 5.9393(5), b = 33.056(2), c = 7.3071(6) β = 102.924(8), 1398.26(19), 4	0.1267, 2420, 174	0.0663, 0.1771, 1.065

dx.doi.org/10.1021/cg200030s |*Cryst. Growth Des.* 2011, 11, 1821–1834

Table 1. Continued

(1*R*,2*S*)(−)-methylephedrinium salts						(±)-methylephedrinium salts					
salt form	chemical formula, MW	space group	cell parameters (Å, °, Å^3), Z	R_{int}, N_{ref}, NV	R_1, wR_2, S	salt form	chemical formula, MW	space group	cell parameters (Å, °, Å^3), Z	R_{int}, N_{ref}, NV	R_1, wR_2, S
H1 methanesulfonate	$C_{11}H_{18}NO$, CH_3O_3S 275.36	$P2_12_12_1$	a = 5.8796(6), b = 21.637(3), c = 33.840(4), 4305.0(9), 12	0.0676, 7305, 502	0.0963, 0.2209, 1.073	**H2** methanesulfonate	$C_{11}H_{18}NO$, CH_3O_3S 275.36	$P2_1$	a = 5.7618(3), b = 17.4809(11), c = 13.7006(8), β = 95.417(5), 1373.78(14), 4	0.0401, 4681, 347	0.0387, 0.0727, 0.804
I1 hydrogen sulfate monohydrate	$C_{11}H_{18}NO$, HO_4S, H_2O 295.35	$P2_12_12_1$	a = 6.0452(4), b = 13.2486(7), c = 18.0074(9), 1442.22(14), 4	0.0438, 3146, 202	0.0495, 0.0864, 1.040	**I2** hydrogen sulfate monohydrate	$C_{11}H_{18}NO$, HO_4S, H_2O 295.35	$P2_1/c$	a = 5.8927(2), b = 17.3398(5), c = 14.4396(4), β = 108.546(2), 1398.79(7), 4	0.0537, 3053, 195	0.0523, 0.1100, 1.083
J1 hydrogen maleate	$C_{11}H_{18}NO$, $C_4H_3O_4$ 295.33	$P2_12_12$	a = 19.9658(5), b = 13.5075(4), c = 5.7764(2), 1557.83(8), 4	0.0620, 3760, 206	0.0421, 0.0886, 0.912	**J2** hydrogen maleate	$C_{11}H_{18}NO$, $C_4H_3O_4$ 295.33	$P2_1/c$	a = 10.6674(7), b = 24.5551(18), c = 5.9212(3), β = 100.111(6), 1526.91(7), 4	0.0890, 2885, 205	0.0421, 0.1062, 0.897
K1 hydrogen malonate	$C_{11}H_{18}NO$, $C_3H_3O_4$ 283.32	$P1$	a = 7.8391(5), b = 7.6967(5) c = 11.2005(7), α = 103.351(5), β = 100.240(5), γ = 111.083(5), 740.34, 1	0.0530, 6411, 389	0.0512, 0.1176, 0.955	**K2** hydrogen malonate	$C_{11}H_{18}NO$, $C_3H_3O_4$ 283.32	$P\bar{1}$	a = 10.194(5), b = 5.708(3), c = 13.204(5), α = 71.637(5), β = 80.822(5), γ = 81.117(5), 715.4(5), 2	0.0517, 2848, 196	0.0524, 0.1665, 1.098
L1 bromide	$C_{11}H_{18}NO$, Br 260.17	$P2_12_12_1$	a = 7.28510(10), b = 9.6672(2), c = 17.2535(3), 1215.10(4), 4	0.0275, 2904, 139	0.0161, 0.0347, 1.023	**L2** bromide	$C_{11}H_{18}NO$, Br 260.17	$P2_1/c$	a = 5.738(5), b = 30.598(5), c = 6.982(5), β = 106.920(5), 1172.8(13), 4	0.0344, 2529, 138	0.0484, 0.0876, 1.396
M1 chloride	$C_{11}H_{18}NO$, Cl 215.71	$P2_12_12_1$	a = 7.1557(2), b = 9.5708(2), c = 16.8627(4), 1154.85(5), 4	0.0300, 3039, 139	0.0267, 0.0598, 0.984	**M2** chloride	$C_{11}H_{18}NO$, Cl 215.71	$C2/c$	a = 33.6032(13), b = 6.9855(2), c = 9.9089(3), β = 95.085(2), 2316.81(13), 8	0.0578, 2659, 139	0.0400, 0.0933, 1.064

dx.doi.org/10.1021/cg200030s |*Cryst. Growth Des.* 2011, 11, 1821–1834

Table 2. Summary of Crystal Data for Four Salt Pairs Where a Difference in Chemical Identity Was Found

(1*R*,2*S*)(−)-methylephedrinium salts						(±)-methylephedrinium salts					
salt form	chemical formula, MW	space group	cell parameters (Å, °, Å^3), *Z*	R_{int}, N_{ref}, NV	R_1, wR_2, *S*	salt form	chemical formula, MW	space group	cell parameters (Å, °, Å^3), *Z*	R_{int}, N_{ref}, NV	R_1, wR_2, *S*
N1 3-chlorobenzoate monohydrate	$C_{11}H_{18}NO$, $C_7H_4ClO_2$, H_2O 353.83	$P2_12_12_1$	*a* = 6.6465(2), *b* = 11.9973(5), *c* = 23.0394(10), 1837.16(12),4	0.0294, 4448, 237	0.0346, 0.0592, 0.865	**N2** 3-chlorobenzoate	$C_{11}H_{18}NO$, $C_7H_4ClO_2$ 335.82	*C*2/*c*	*a* = 24.7872(12), *b* = 5.8486(2), *c* = 23.7079(11), β = 97.920(4), 3404.2(3), 8	0.0508, 4333, 219	0.0403, 0.0949, 0.936
O1 benzoate monohydrate	$C_{11}H_{18}NO$, $C_7H_5O_2$, H_2O 319.39	$P2_12_12_1$	*a* = 8.6280(2), *b* = 10.9921(2), *c* = 18.7914(4), 1782.17(6), 4	0.0253, 4075, 227	0.0309, 0.0595, 0.916	**O2** benzoate	$C_{11}H_{18}NO$, $C_7H_5O_2$ 301.37	*Pbca*	*a* = 13.9277(3), *b* = 11.2200(3), *c* = 20.7001(7), 3234.78(16), 8	0.0350, 3168, 210	0.0325, 0.0734, 0.924
P1 iodide, tri-iodide	$2C_{11}H_{18}NO$, I, I_3 434.06	$P2_1$	*a* = 7.6416(2), *b* = 25.5067(5), *c* = 7.8781(2), β = 104.173(3), 1488.80(6), 4	0.0452, 7001, 291	0.0462, 0.0668, 1.136	**P2** iodide	$C_{11}H_{18}NO$, I 307.16	$P\bar{1}$	*a* = 7.6216(4), *b* = 7.6754(4), *c* = 11.0946(5), α = 83.537(4), β = 84.005(5), γ = 70.642(5), 606.88(5), 2	0.0236, 2549, 138	0.0189, 0.0403, 0.970
Q1 4-hydroxybenzene-sulfonate	$C_{11}H_{18}NO$, $C_6H_5O_4S$ 353.42	$P2_1$	*a* = 6.13990(10), *b* = 13.3725(4), *c* = 10.3002(3), β = 98.217(2), 837.02(4), 2	0.0334, 3749, 233	0.0316, 0.0783, 1.092	**Q2** 4-hydroxybenzene-sulfonate hemihydrate	$C_{11}H_{18}NO$, $C_6H_5O_4S$, $0.5H_2O$ 362.43	$P\bar{1}$	*a* = 10.2179(3), *b* = 13.6409(4), *c* = 15.0037(4), α = 64.086(3), β = 87.575(2), γ = 72.856(2), 1788.26(9), 4	0.0387, 8578, 480	0.0367, 0.0842, 0.940

dx.doi.org/10.1021/cg200030s |*Cryst. Growth Des.* 2011, 11, 1821–1834

Table 3. Summary of Crystal Data for Compounds Where the Racemic Compound Was Found To Form As a Conglomerate

(1*R*,2*S*)(−)-methylephedrinium salts						(±)-methylephedrinium salts	
salt form	chemical formula, MW	space group	cell parameters (Å, °, Å^3), *Z*	R_{int}, N_{ref}, NV	R_1, wR_2, *S*	salt form	
R1 4-hydroxybenzoate	$C_{11}H_{18}NO$, $C_7H_5O_3$ 317.37	$P2_1$	*a* = 12.8247(5), *b* = 7.7239(3), *c* = 18.0650(8), *β* = 104.569(4) 1731.92(12), 4	0.0371, 7264, 445	0.0439, 0.0775, 0.878	**R2** 4-hydroxybenzoate	crystallizes as a conglomerate, same parameters as R1
S1 4-chlorobenzoate	$C_{11}H_{18}NO$, $C_7H_4ClO_2$ 335.82	$P2_1$	*a* = 5.99150(10), *b* = 14.2038(3), *c* = 9.9003(2), *β* = 96.6790(10), 836.82(3), 2	0.0369, 3696, 214	0.0408, 0.1033, 1.189	**S2** 4-chlorobenzoate	crystallizes as a conglomerate, same parameters as S1
T1 *p*-toluate	$C_{11}H_{18}NO$, $C_8H_7O_2$ 315.40	$P2_1$	*a* = 6.0437(2), *b* = 14.1258(3), *c* = 9.9363(3), *β* = 98.017(3), 839.99(4), 2	0.0285, 4515, 220	0.0340, 0.0682, 0.949	**T2** *p*-toluate	crystallizes as a conglomerate, same parameters as T1

dx.doi.org/10.1021/cg200030s |*Cryst. Growth Des.* 2011, 11, 1821–1834

Table 4. Graph-Set Analysis for Chemically Identical Salt Pairs of Benzoate Derivatives (a-anion, c-cation, w-water)[a]

compound	hydrogen bond		graph-set		network growth	compound	hydrogen bond		graph-set		network growth
A1	a	$OH_c\cdots COO^-$	>a < b	$C_2^2(9)$	*a*	**A2**	a	$OH_c\cdots COO^-$	>a < b	$C_2^2(9)$	*a*
	b	$NH\cdots COO^-$					b	$NH\cdots COO^-$			
B1	a	$OH_c\cdots COO^-$	>b < c	$D_1^2(2)$	*a*	**B2**	a	$OH_c\cdots COO^-$	>b < c	$D_2^2(2)$	*b*
	b	$NH\cdots COO^-$	>a < c	$D_2^2(5)$			b	$NH\cdots COO^-$	>a < c	$D_2^2(5)$	
	c	$OH_w\cdots COO^-$	>a < d	$D_2^2(8)$			c	$OH_w\cdots COO^-$	>a < d	$D_2^2(8)$	
	d	$OH_w\cdots NO_2$	>b < d	$D_2^2(8)$			d	$OH_w\cdots NO_2$	>b < d	$D_2^2(8)$	
			>a < b	$C_2^2(9)$					>a < b	$C_2^2(9)$	
			>c < d	$C_2^2(9)$					>c < d	$C_2^2(9)$	
C1	a	$OH_c\cdots COO^-$	>a < b	$C_2^2(9)$	*a*	**C2**	a	$OH_c\cdots COO^-$	>a < b	$C_2^2(9)$	*b*
	b	$NH\cdots COO^-$					b	$NH\cdots COO^-$			
D1	a	$OH_c\cdots COO^-$	>c < d	$C_2^2(9)$	*a*	**D2**	a	$OH_c\cdots COO^-$	>a < b	$C_2^2(9)$	*a*
	b	$NH\cdots COO^-$	>a < b	$R_2^2(9)$			b	$NH\cdots COO^-$			
	c	$OH_c\cdots COO^-$									
	d	$NH\cdots COO^-$									
E1	a	$OH_c\cdots COO^-$	>a < b	$C_2^2(9)$	*b*	**E2**	a	$OH_c\cdots COO^-$	>a < b	$C_2^2(9)$	*b*
	b	$NH\cdots COO^-$					b	$NH\cdots COO^-$			

[a] The entry under "network growth" gives the crystallographic direction in which the hydrogen-bonding network propagates. Graph-set analysis for the other salts is presented in the Supplementary Information.

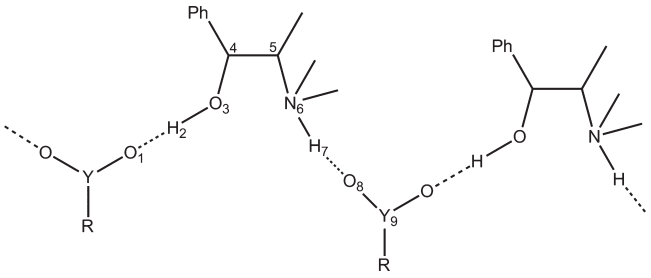

Figure 3. Schematic of the common $C_2^2(9)$ graph set motif. Y = C or SO.

rather than iodide counterions) and three cases where the racemic salt spontaneously resolved to form a conglomerate. Three spontaneous resolutions from 20 are slightly higher than the often quoted 5−10% occurrence of this phenomenon but fits with the suggestion that salt forms are more prone to spontaneously resolve than neutral molecules.[4,18] Also of note here is that in our hands the free base itself spontaneously resolves to form a conglomerate.

There are several features general to all 37 independent crystal structures. All form hydrogen-bonded cation−anion pairs, but there are no direct cation−cation hydrogen-bonded pairs. Anion−anion hydrogen-bonding interactions are present in all structures with an organic anion that possesses a classic hydrogen-bond donor. The salt structures containing hydrogen-maleate and hydrogen-malonate anions conform to Etter's rules,[16] which predict that intramolecular bonds will form in preference to intermolecular bonds, as all use their COOH groups as internal hydrogen-bond donors. Of the 37 structures, six were isolated as monohydrates and one as a hemihydrate. In all structures except the two ethane-1,2-disulfonate salts G1 and G2, the acid and base react to give a one to one salt. In the ethane-1,2-disulfonate structures, the acid is dideprotonated and thus two to one cation to anion salts are produced. None of the reported products have neutral free acid molecules present, and so all are true salts and not cocrystals.

To aid further discussion, the structures will be separated into groups depending on their counterion type and initially discussed in terms of structure similarities through graph set analysis and network growth. The structures will also be analyzed to determine different cation conformations and crystal packing similarities throughout the data set. Finally, the melting points and densities will be examined to see if the pairs of chemically identical salts conform to Wallach's rules.

Substituted Benzoate Salts. There are five salt pairs with benzoic acid derived counterions, which crystallize to produce chemically identical species for the (1*R*,2*S*)(−)-methylephedrinium and (±)-methylephedrinium salts. The crystallographic details are shown in Table 1, compounds A1 to E2. The graph set analysis for these five pairs is shown in Table 4. A common feature is that all contain the $C_2^2(9)$ motif, see Figure 3, involving the cation's OH and NH groups as donors and both O-atoms of the anion COO^- group as the acceptors. All 10 structures grow using the $C_2^2(9)$ chain to give one-dimensional (1D) hydrogen-bonded networks, either along the crystallographic *a* or crystallographic *b* directions; see Figure 4. Comparison of the hydrogen-bonding details shows that the enantiopure-racemic pairs all have identical graph-set analyses for each salt pair, except that of 4-nitrobenzoate (D1 and D2). This latter difference is related to the fact that there are two anions and two cations present per asymmetric unit of D1. The carboxylate group of one anion forms hydrogen bonds with the NH and OH of two different cations, while the crystallographically independent anion interacts with NH and OH functionalities of a single methylephedrinium. Thus, the structure contains both ring, $R_2^2(9)$, and chain, $C_2^2(9)$, motifs, see Figure 5, and the $C_2^2(9)$ chain is present in all 10 of these benzoate salt structures. Kinbara et al. reported that they found significant differences in the hydrogen-bonding motifs adopted between enantiopure and racemic primary amines and carboxylate anions.[11b] We do not observe the same specific hydrogen-bonding motif, nor significantly do we see any systematic difference between the enantiopure and chiral salts with respect to hydrogen-bonding motifs.

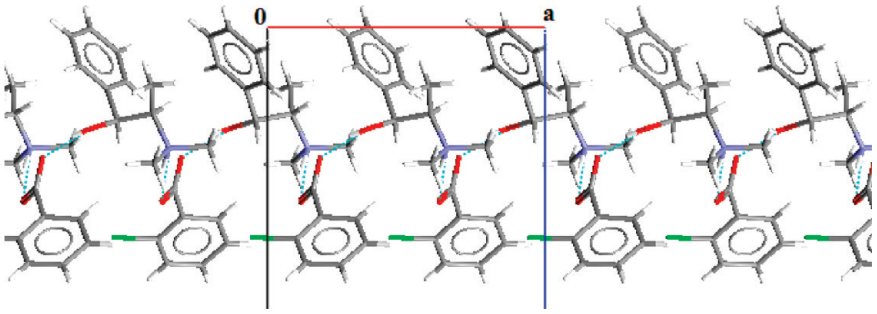

Figure 4. Growth of a 1D hydrogen-bonded $C_2^2(9)$ chain in the *a* direction for (1*R*,2*S*)(−)-methylephedrinium 2-chlorobenzoate.

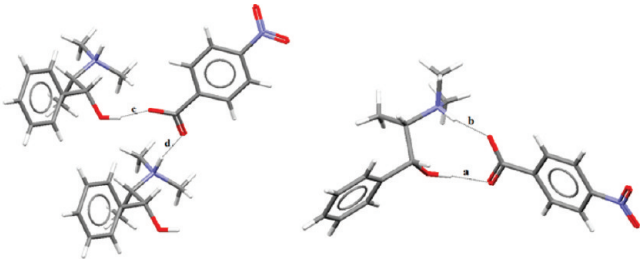

Figure 5. Illustration of the $C_2^2(9)$ and $R_2^2(9)$ graph-sets found for (1*R*,2*S*)(−)-methylephedrinium 4-nitrobenzoate.

Seven further benzoate-based salt structures are available here for comparison. In the three conglomerate forming cases R, S, and T where only the enantiopure structure was accessible, the common $C_2^2(9)$ chain was observed as above. Note that only four *para* substituted benzoates were used here and that it was three of these four that formed conglomerates. Only the nitro derivative formed a racemic phase, while the chloro, hydroxyl, and methyl derivatives showed spontaneous resolution. The implication is that similarly shaped counterions all behaved in like manner with respect to spontaneous resolution.

In a further four cases, enantiopure and racemic benzoate structures are available, but these salts did not form chemically identical pairs. The enantiopure species are monohydrates, while the racemic compounds are anhydrous (see Table 2 compounds N1 to O2) and as such identical hydrogen-bonding motifs are not seen for the enantiopure-racemic pairs. However, there are similarities to the previously discussed structures. The structures of (±)-methylephedrinium 3-chlorobenzoate, (1*R*,2*S*)(−)-methylephedrinium benzoate monohydrate and (±)-methylephedrinium benzoate all grow to form 1D ribbons via the $C_2^2(9)$ chain as seen before. However, (1*R*,2*S*)(−)-methylephedrinium 3-chlorobenzoate monohydrate (N1) forms a two-dimensional (2D) sheet with network growth in a second direction through solvent separated anions along the crystallographic *a* direction forming a $C_2^2(6)$ chain; see Figure 6. This structure is thus different from all other benzoate salts studied herein, in that it does not form direct N−H···OOC hydrogen-bonds. Indeed, N1 is even more of an outlier, in that all of the other salts in this paper make direct hydrogen bonds between NH and the formally charged group of the anion.

Sulfonate and Hydrogen-Sulfate Salts. Of the five enantiopure-racemic pairs of YSO_3^- (Y = R or OH) salt structures obtained, four are of pairs of salts that are chemically identical. However, the graph-set analysis detailed in the Supporting Information shows that only the salts of benzenesulfonate

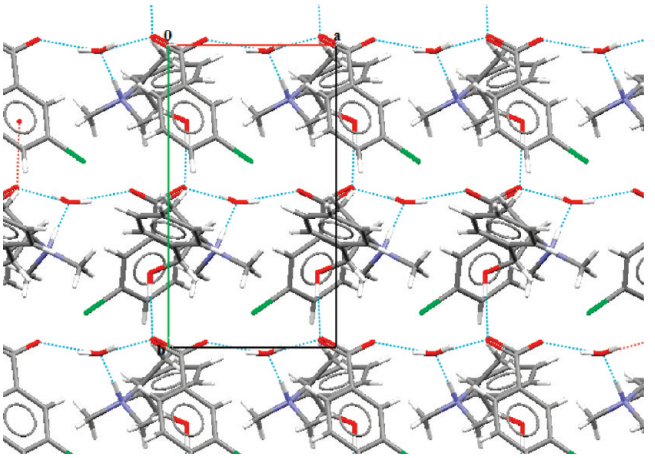

Figure 6. Hydrogen-bonds propagate in the *a* and *b* directions, forming a 2D sheet in (1*R*,2*S*)(−)-methylephedrinium 3-chlorobenzoate.

(F1 and F2) have the same hydrogen-bonding present for both structures of the pair. This is in direct contrast to what was found for the benzoate salts. One similarity throughout 9 of the 10 structures (the four chemically identical paired structures and (1*R*,2*S*)(−)-methylephedrinium 4-hydroxybenzenesulfonate, Q1) is that only two of the three sulfonate oxygen atoms (or three of the four sulfate oxygen atoms) are utilized as hydrogen-bond acceptors. This allows for a $C_2^2(9)$ graph-set to be present as the means of network propagation for the salts of benzenesulfonate, 1,2-ethanedisulfonate, and hydrogen sulfate monohydrate. Despite the change from COO to RSO_3 functionality, this motif is analogous to the $C_2^2(9)$ chain seen with the benzoate salts. However, the methanesulfonate salts do not have the $C_2^2(9)$ chain present and instead display discrete $D_2^2(8)$ motifs. Only for the structure of (±)-methylephedrinium 4-hydroxybenzenesulfonate hemihydrate, Q2, are all crystallographically independent sulfonate oxygen atoms involved in hydrogen bonding.

The crystal structure for compound (1*R*,2*S*)(−)-methylephedrinium 1,2-ethanedisulfonate, G1, has two base molecules per asymmetric unit compared to one per asymmetric unit for the equivalent (±)-methylephedrinium salt, G2. The structure of G2 forms hydrogen bonds with two cations and two anions in a ring formation, $R_4^4(24)$; see Figure 7. In the G1 structure, instead of the hydrogen-bonding forming a ring, the ethanedisulfonate ion lies along the crystallographic *a* direction and forms a second $C_2^2(9)$ chain making the overall network a two-dimensional (2D) sheet. This formation of a ring is also seen in the structure of (±)-methylephedrinium hydrogen-sulfate monohydrate where the

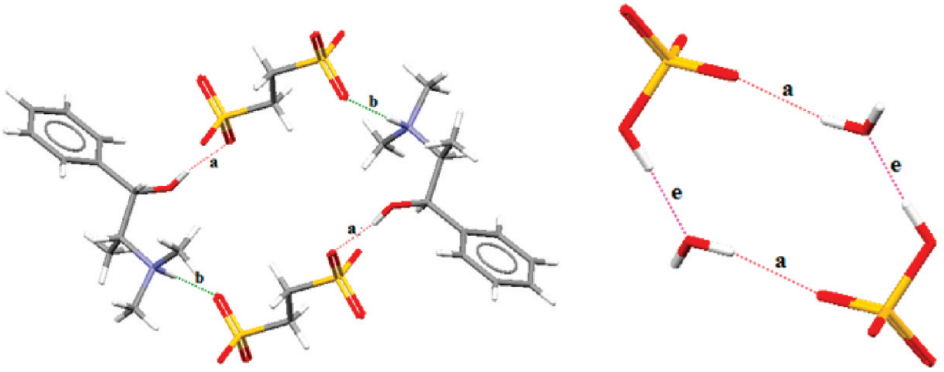

Figure 7. Ring formation in (±)-methylephedrinium 1,2-ethanedisulfoante, $R_4^4(24)$, and (±)-methylephedrinium hydrogen-sulfate monohydrate, $R_4^4(12)$.

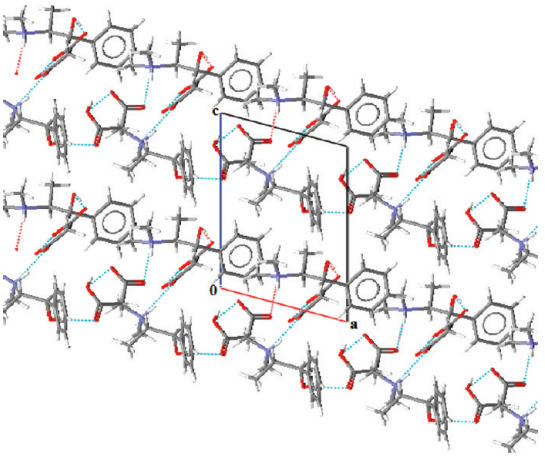

Figure 8. Propagation of of hydrogen-bonding in (1*R*,2*S*)(−)-methylephedrinium malonate along the crystallographic *a* direction.

anions and water molecules hydrogen bond to form two $R_4^4(12)$ rings; see Figure 7.

Dicarboxylic Acid Derivatives. We describe two enantiopure-racemic pairs of dicarboxylic acid salt structures and both are chemically identical, namely, the hydrogen-maleate and hydrogen-malonate salts. The two hydrogen-maleate salts (J1 and J2) have identical hydrogen-bonding present, with the hydrogen-malonates' hydrogen-bonding differing due to the (1*R*,2*S*)(−)-methylephedrinium malonate salt having two ion pairs per asymmetric unit, which results in the growth of two parallel units along the crystallographic *a* direction; see Figure 8. All four salts conform to Etter's rules,[16] with the presence of internal hydrogen bonds giving the graph-sets $S_1^1(7)$ and $S_1^1(6)$. The common $C_2^2(9)$ chain seen for both the benzoate derivatives and the sulfonate salts is absent here. This is because one of the oxygen atoms of the carboxylate is involved in intramolecular hydrogen bonding. In the case of the hydrogen-maleate salts, $C_2^2(12)$ chains propagate through using the oxygen atoms at either end of the maleate anion. The hydrogen-malonate pairs have different hydrogen bonding from each other, with the enantiopure salt showing a discrete graph-set and the racemic salt propagating through $C_2^2(7)$ chains with both the NH and OH of the cation hydrogen bonding to the same oxygen of the anion.

Halide Salts. Three pairs of halide salt structures were obtained. For the chloride and bromide salts, the enantiopure and racemic salt pairs are chemically identical. The "iodide" salts differ as the (1*R*,2*S*)(−)-methylephedrinium salt is a mixed iodide, tri-iodide structure, while the racemic salt was isolated as the simple iodide. The bromide and chloride pairs form identical hydrogen-bonding patterns and all six propagate via a $C_2^1(7)$ chain. All, excluding the iodide-tri-iodide structure, form 1D ribbons. In the (1*R*,2*S*)(−)-methylephedrinium iodide tri-iodide structure, P1, network propagation is in the *a* and *c* directions via $C_2^1(7)$ chains, giving the same hydrogen-bond motif as present in the other halides. The tri-iodide anions form channels but make no hydrogen-bonding interactions, as illustrated in Figure 9.

Different Conformations of the Cation. Within the salt structures the cation adopts one of three different conformations. These three different conformations are illustrated in Figure 10. Four torsion angles can be used to describe these conformations, and these encompass the two stereocenters at carbon atoms C7 and C8. Between each of the three classes, significant variation is based largely on torsion angle 4. Overlay of the cations that represent the three different conformations was performed using the structural overlay feature in Mercury CSD 2.3.[17] This is illustrated in Figure 11 and further details are tabulated in the Supporting Information. Of those structures where more than one crystallographically independent cation exists in the asymmetric unit, only G1 contains two different conformers. Conformation (a) is the most common, being present in 23 cations, with a torsion angle 4 range of −26.27 (in D1) to −63.75° (in L2). Conformation (b) occurs in 16 of the cations and has a range of 67.19 (in F2) to 91.29° (in J2). Conformation (c) is the least reoccurring, being present in only seven cations and has a torsion angle 4 range of 175.65 (in T1) to −170.62° (in G1). Interestingly, only arrays of enantiopure cations exist in this third conformation, that with the amine proton *anti* to the phenylethylene chain. Related work on ephedrine salts found two cation conformations.[11d,12a,18]

Crystal Packing Similarities. Investigation into similarities in the crystal packing of the 37 structures was performed by using the "crystal packing similarity" module in Mercury CSD 2.3.[17] This tool takes a reference molecule and then examines the three-dimensional (3D) geometry of the cluster of surrounding molecules; this then allows the program to determine the number of similar molecules within clusters from several structures, and their geometric similarity. An excellent description of this technique is given in ref 19. Analysis was performed for the group of 37 structures and the results are summarized in the tree diagram, Figure 12. This was constructed by looking for similar

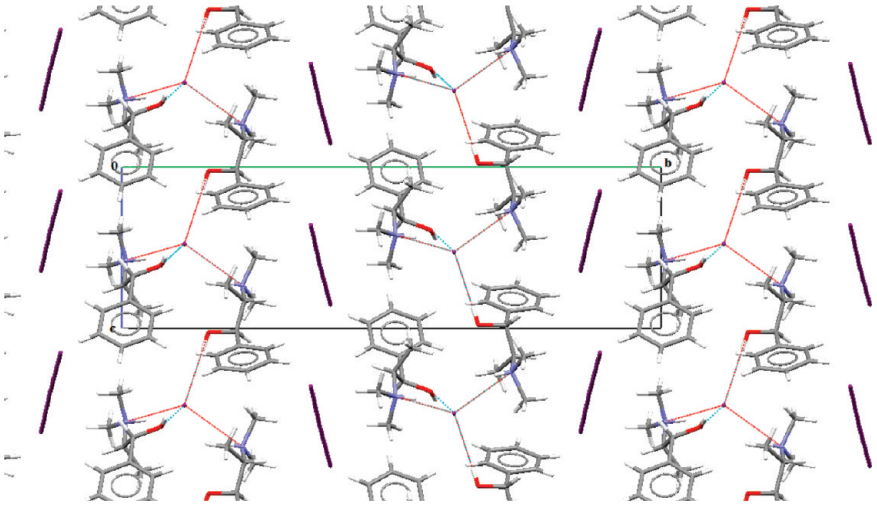

Figure 9. Network growth along the *c* direction for (1*R*,2*S*)(−)-methylephedrinium iodide tri-iodide. View is down the *a* axis. The tri-iodide anions are shown as purple bars.

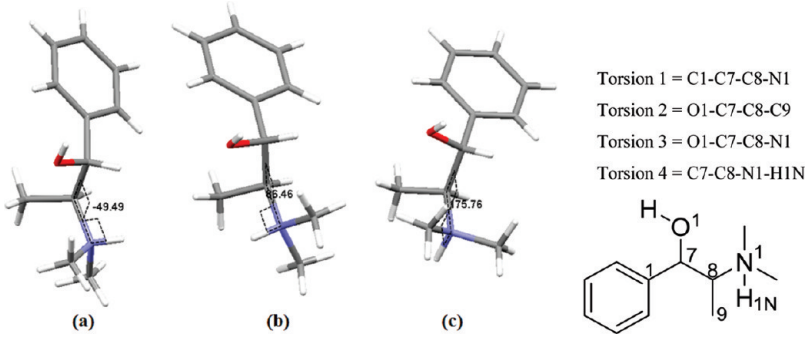

Figure 10. Three conformations were found for the methylephedrinium cation. Conformation (a) is illustrated by compound A1, (b) by H1, and (c) by N1.

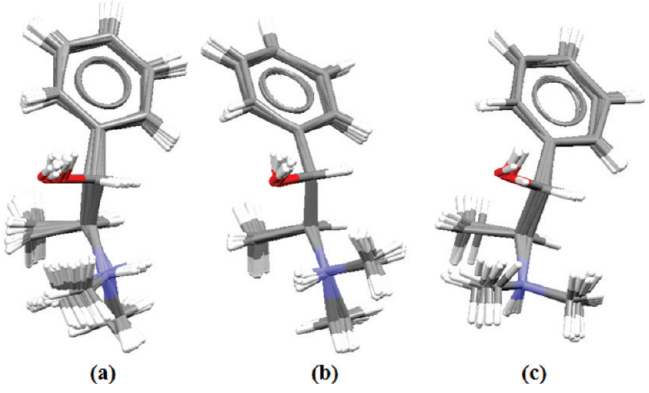

Figure 11. (a−c) Overlays of the three different cation conformations.

packing in various cluster sizes ranging from 2 to 15 cations. Note that the analysis looked only at the largest molecular component of the salts, that is, the cation, in order to exclude interference from the various anions and water molecules, with a distance and torsion angle tolerance of 20%.[19] Structures that have 15 out of 15 similar molecules within a structure are considered to be isostructural, at least with respect to cation packing.

In the tree diagram, less similar structures are named at the top of the diagram with the similarity increasing on moving downward. The tree branches convey similar substructures. The colors of the large circles highlight different cation molecular conformations, as discussed above, to show reoccurrences throughout the tree. The small colored dots indicate distinct cation to cation pair geometries, or packing motifs. As can be seen from the tree diagram all but four structures (highlighted with small green dots) have a common packing motif for two cations. The three different packing motifs are illustrated in Figure 13, as motif X (2_1 conformer, yellow dots), motif Y (translation conformer, blue dots), and motif Z (racemic conformer, red dots). Motif Y, the "translation conformer" is by far the most common, occurring in 28 of the structures, with the "racemic conformer" Z occurring in 3 structures, and the "2_1 conformer" X occurring in only 2 isostructural structures. The remaining four structures, K1, M2, O1 and O2, are outliers in the data set and do not fit into any of the three different groups and also do not relate to each other. All of the three different cation molecular conformations observed are able to adopt the "translation conformer," with the other two packing motifs being adopted only by cations with molecular conformation (a).

The tree diagram shows that there are several structures that are isostructural with respect to cation packing. These structures are located at the bottom of the tree with 15 matching neighbors

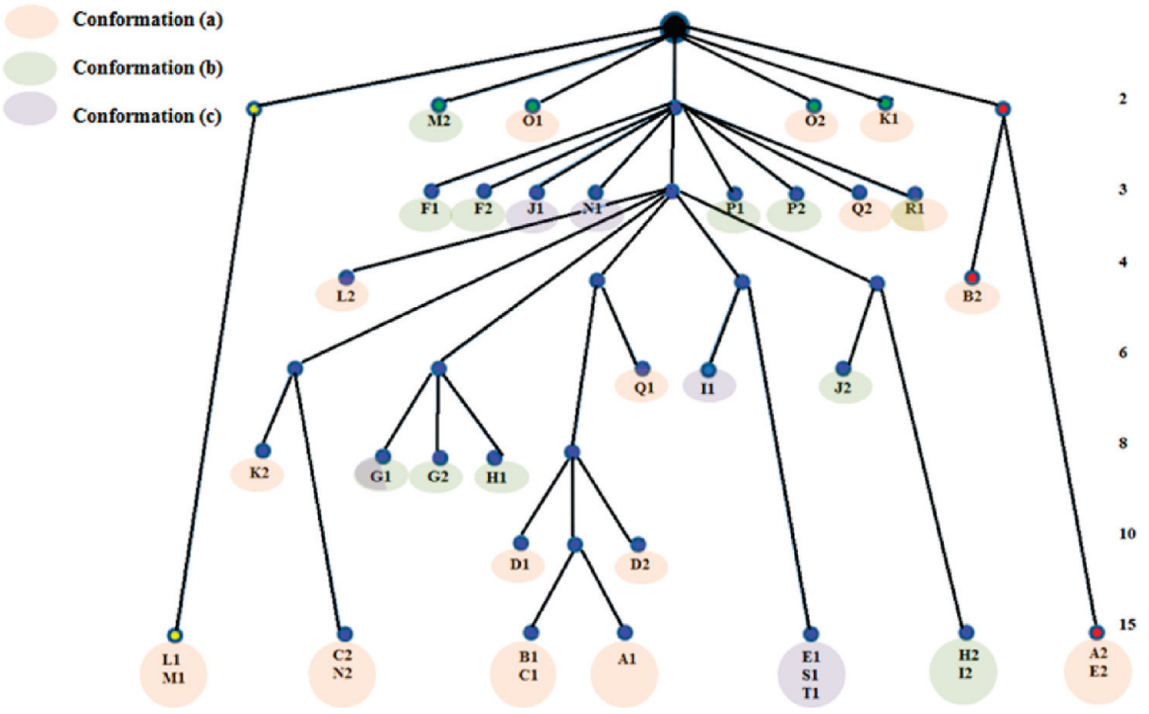

Figure 12. Tree diagram generated from crystal packing similarity search on the cation fragment.

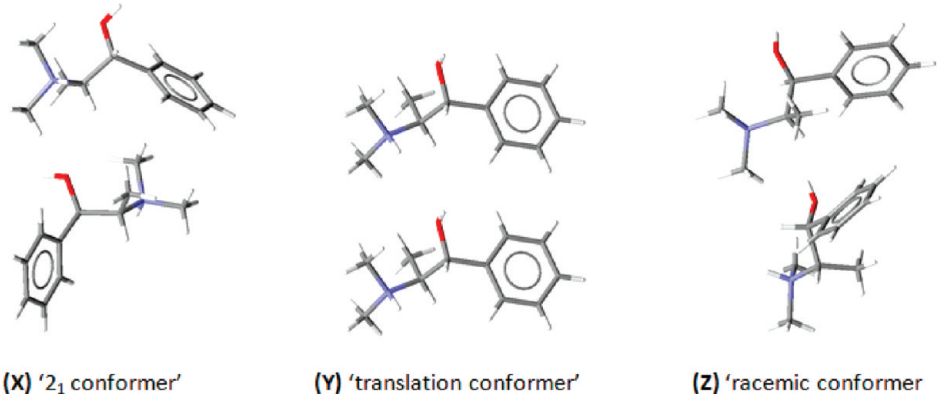

Figure 13. Pair-packing conformations observed for cations.

in the similarity packing search. Four of the six isostructural groups (those of compounds L1, M1, C2 N2, E1 S1 T1, and A2 E2) have both identical orientations of the cations and identical hydrogen-bonding present within the structures. However, within the isostructural pair B1 and C1 the anion orientation is different; see Figure 14. This allows the 2-nitrobenzoate structure B1 to also accommodate a water molecule. The additional water molecule results in additional hydrogen bonds being present, as well as the $C_2^2(9)$ chain. These additional interactions with the water molecule do not result in an additional dimension of network propagation; instead, an anion−water−anion motif gives an additional $C_2^2(9)$ chain parallel to the first. Finally, for the isostructural pair of H2 and I2 ($MeSO_3$ and SO_4H anions) the addition of a water molecule and extra hydrogen-bonding capability in I2 gives a significant change in hydrogen bonding. This results in a 3D network for the hydrogen-sulfate monohydrate structure, compared to the more common 1D motif of the methanesulfonate structure. The analysis of structures B1, C1, H2, and I2 suggests that here hydrogen bonding is a consequence of the cation crystal packing array and not the other way around. This conclusion was reached as the cation packing is isostructural and does not change despite the addition of water molecules and major alterations to the hydrogen-bonding motifs.

Density Comparisons of Identical Salt Pairs. Comparison of the densities and melting points of the enantiopure and racemic salt pairs has been attempted only for the 13 pairs that form chemically identical salts, Figure 15. The average density of the enantiopure salts is 1.300 g/cm^3, whereas the average density for the racemic salts is approximately 1.5% greater at 1.319 g/cm^3. This is in line with previous studies.[9] However, looking individually at the 13 salt pairs, only 7 conform to Wallach's rules,[7] where the racemic compound is more dense than the enantiopure compound. Of the remainder, there are four pairs where the density is effectively identical (differences of less than 0.005 g/cm^3) and two salt pairs (2-nitrobenzoate and

dx.doi.org/10.1021/cg200030s |*Cryst. Growth Des.* 2011, 11, 1821–1834

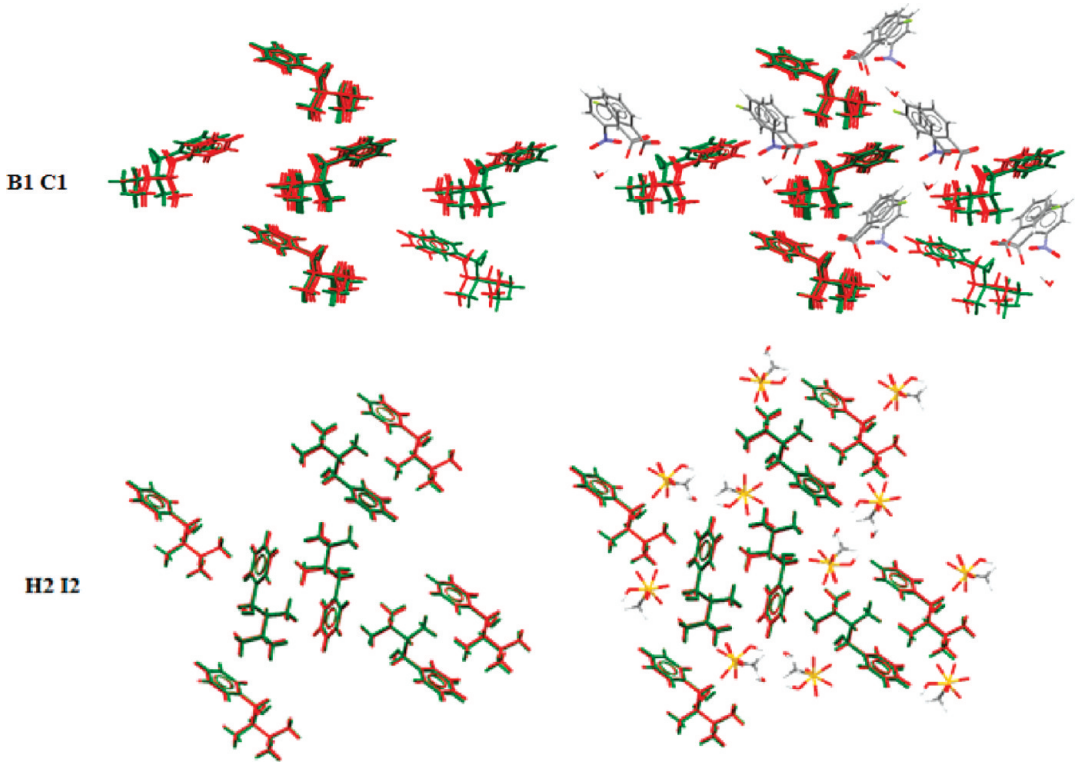

Figure 14. Comparison of packing for isostructural pairs, shown both with (right-hand side) and without (left-hand side) the anion present. Green and red indicate cations from different structures.

1,2-ethanedisulfate, samples B and G) where the enantiopure compound is considerably denser than the racemic compound. Interestingly, H2, here the only racemic salt to crystallize in a chiral space group, does obey Wallach's rule. Note that in all cases here, slow crystallization of the racemic compound gave only racemic crystalline phases — implying that the racemic phase is thermodynamically more stable than the enantiopure phase. To investigate potential structural reasons for the exceptions to Wallach's rule, compounds B and G were examined for differences between their structures and those of the other salts. Of the 13 chemically identical pairs, G is unique in being the only one with a significant difference in hydrogen bonding between its enantiopure and racemic forms; see graph-set analysis in the Supporting Information. Note that the hydrogen bonding in enantiopure G1 propagates in two dimensions rather than the 1D chain seen for G2. We suggest that this difference in hydrogen bonding lies at the root of the observed difference in packing efficiency. This ties in with previous suggestions that significant differences in hydrogen bonding may lie at the root of observed differences in behavior of racemic and enantiopure salts.[11b] However, B1 and B2 have identical hydrogen-bonding motifs (the common $C_2^2(9)$ graph set) so differences in hydrogen bonding is not the explanation here. B is somewhat unusual in being one of only two hydrates in the group of 13 pairs, but potentially of more interest is that B2 is one of the three structures that adopt the "Z" racemic cation pair packing motif. The other two "Z" motifs are for A2 and E2. Interestingly, both of these structures are in the group with essentially identical densities for the enantiopure and racemic structures. This suggests that the racemic packing motif Z is less packing efficient than the homochiral motifs X and Y. Packing efficiencies in both compounds B and G are illustrated by the void calculations shown in Supporting Information. A final point is that the three conglomerate forming compounds, R1, S1, and T1, do not appear to have enantiopure phases with significantly higher densities than those of comparable species. Indeed, the density of R1 (1.217 g/cm^3) is the lowest recorded here. Thus, the "extra" stability of these salts is not reflected in their densities.

Melting Point Comparisons of Identical Salt Pairs. Melting point is a simple parameter of interest both as a crucial material characteristic for working and tableting pharmaceutical compounds[1] and as a feature correlated to other vital parameters such as lattice energy and solubility.[11d,12,20] Experimental melting points could only be achieved for 12 of the 13 identical salt pairs, as both the salts of methanesulfonate were hygroscopic and therefore a reliable value could not be measured. The average melting point for the 12 enantiopure salts is 127.0 °C, with the average racemic melting point being greater with a value of 133.0 °C. This is consistent with the racemic phases being thermodynamically favored over the enantiopure phases. Individual pair-evaluation indicates that the melting point is higher for the racemic compound in 8 of 12 cases. However, the exceptional samples are not all the same as those identified by the density measurement comparison, as illustrated in Figure 15. The compounds B and G were highlighted above as having significantly higher densities for the enantiopure compound. Of these, only the 1,2-ethanedisulfonate salts also have a higher melting point for the enantiopure salt, G1, over its racemic equivalent, G2. G1 and G2 were the compounds where a change in hydrogen-bonding motif (and network dimensionality) was noted. However, for B the racemic compound has a much higher melting point than the enantiopure form. Care needs to be taken here as the B salts are hydrates, and the melting points recorded will presumably be those of anhydrous forms of unknown structure. The 3-fluorobenzoate salts C1 and C2 are the other

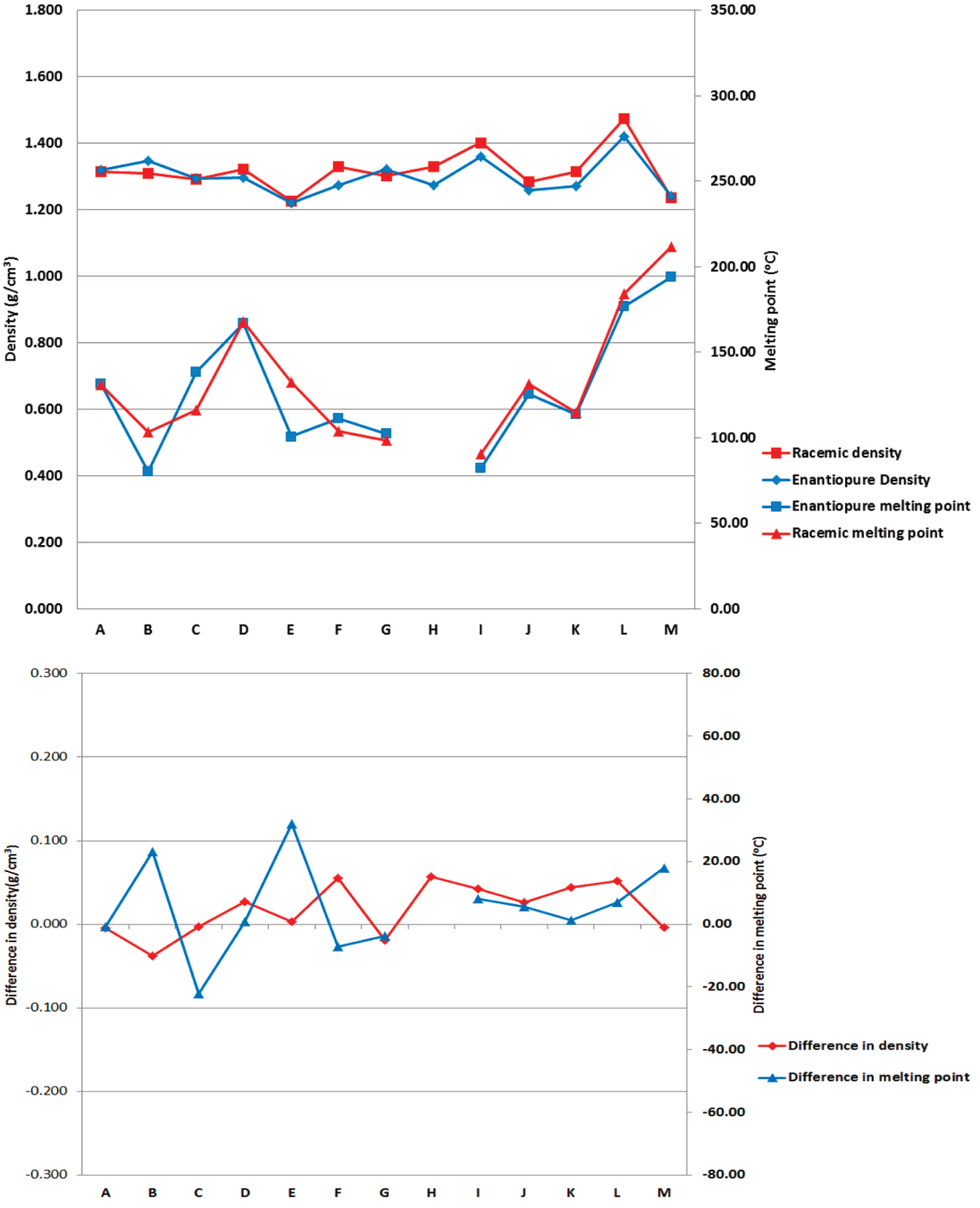

Figure 15. Density and melting points of 13 identical salt pairs. Top diagram shows absolute values; bottom diagram shows differences.

pair to have a much higher melting point for the enantiopure form than the chiral form. The structural analysis sheds little light on this, but it should be noted that C1 and C2 have essentially identical densities and thus do not strictly obey Wallach's rule. Thus, it can be said that both pairs that have high melting point enantiopure forms are also observed to disobey Wallach's rule.

CONCLUSION

This paper investigates 20 pairs of enantiopure and racemic methylephedrinium salts. Of the 20 pairs, 13 produced enantiopure and racemic crystal phases of identical chemical makeup, three pairs had racemic species that spontaneously resolved to give conglomerates, and four pairs produced salts that crystallized as different chemical entities. All three of the conglomerates had anions derived from *para*-substituted benzoic acids but did not appear to be structurally different from the other salts or to have exceptionally high densities.

All the structures analyzed formed hydrogen-bonded cation−anion pairs, with no cation−cation pairs present. In all cases except N1, the cation−anion contact involved the cation's NH groups as a hydrogen-bond donor to the anion. The commonest graph-set motif of $C_2^2(9)$ was found to be present in 22 of the 37 independent structures and was flexible enough to include both OCO and OSO functionalities. The equivalent $C_2^1(7)$ motif was present in all six halide structures. Salts of dicarboxylic acids did

dx.doi.org/10.1021/cg200030s |*Cryst. Growth Des.* 2011, 11, 1821–1834

not form the $C_2^2(9)$ motif. The network growth varied with 29 salts producing 1D hydrogen-bonded chains, five salts producing 2D hydrogen-bonded sheets, and three salts producing 3D hydrogen-bonding networks. The methylephedrinium cation is seen to adopt one of three different conformations and there are also three common cation pair packing motifs, with 13 salt structures adopting 6 different 3D isostructural groupings with respect to cation packing. Hydrogen-bonding differences (and indeed differing hydration states) are seen within some of the otherwise isostructural cation arrays.

For the chemically identical enantiopure-racemic pairs, melting points and densities were collated, principally as a test of the validity of Wallach's rules.[7] In general, the overall trend in densities agrees with Wallach's rules with the average racemic density being higher than the average enantiopure density. This though may be a somewhat counterfeit result; we can access crystals in cases where the stability of the enantiopure form is significantly less than that of the racemic form (as enantiopure starting material is available), but we cannot access structures of the racemic form if the enantiopure form is significantly more stable. As our comparison can be made only when both forms are available, there will always be a bias toward more stable (and hence presumably more dense) average values for the set of racemic compounds. Close examination of the individual pairs finds that exceptions to Wallach's rule are common, with 6 of 13 pairs failing to have a more dense racemic structure. Overall, we find little evidence to support the notion that packing racemic ions with achiral ones must give a denser structure than packing enantiopure and achiral ions. One of the three observed cation packing motifs (the racemic motif Z) is closely associated with failure of Wallach's rule but does not explain all the observed instances, for instance, that of compound G, where there is a significant difference between the hydrogen-bonding motifs of G1 and G2. Thus, we have highlighted two different details of array structure that may explain inefficient packing.

■ ASSOCIATED CONTENT

Supporting Information. Details of single crystal characterizations as cif files and details of graph-set analyses, geometries of the three molecular conformations found, tabulated density and melting point data and a graphical comparison of packing efficiency in compounds B and G. This information is available free of charge via the Internet at http://pubs.acs.org.

■ AUTHOR INFORMATION

Corresponding Author

*(A.R.K.) Fax: (+44) 141-548-4822. E-mail: a.r.kennedy@strath.ac.uk (C.A.M.) Fax: (+44)141-548-4822. E-mail: catriona.morrison@strath.ac.uk..

■ ACKNOWLEDGMENT

The authors thank MSD and the EPSRC (CTA fund) for funding towards a studentship for CAM. Thanks are also due to the National Crystallography Service at the University of Southampton for data collection on six of the reported structures.

■ REFERENCES

(1) (a) Stahl, P. H.; Wermuth, C. G., Eds. *Handbook of Pharmaceutical Salts: Properties, Selection and Use*; VHCA: Zurich, 2008. (b) Gould, P. L. *Int. J. Pharm.* **1986**, *33*, 201.

(2) Paulekuhn, G. S.; Dressman, J. B.; Saal, C. *J. Med. Chem.* **2007**, *50*, 6665.

(3) (a) Borman, S. *Chem. Eng. News* **1990**, *68*, 9. (b) Millership, J. S.; Fitzpatrick, A. *Chirality* **1993**, *5*, 573.

(4) Jacques, J.; Collet, A.; Wilen, S. H. *Enantiomers, Racemates, and Resolutions*; Wiley: New York, 1981.

(5) Li, Z. J.; Grant, D. J. W. *J. Pharm. Sci.* **1997**, *86*, 1073.

(6) Kitaigorodskii, A. I. In *Organic Chemical Crystallography*; Consultands Bureau: New York, 1961.

(7) Wallach, O. *Liebigs Ann. Chem.* **1895**, *286*, 90.

(8) Eliel, E. L. *Stereochemistry of Carbon Compounds*; McGraw-Hill: New York, 1962.

(9) Brock, C. P.; Schweizer, W. B.; Dunitz, J. D. *J. Am. Chem. Soc.* **1991**, *113*, 9811.

(10) Brock, C. P.; Dunitz, J. D. *Chem. Mater.* **1994**, *6*, 1118.

(11) (a) Zingg, S. P.; Arnett, E. M.; McPhail, A. T.; Bothnerby, A. A.; Gilkerson, W. R. *J. Am. Chem. Soc.* **1988**, *110*, 1565. (b) Kinbara, K.; Hashimoto, Y.; Sukegawa, M.; Nohira, H.; Saigo, K. *J. Am. Chem. Soc.* **1996**, *118*, 3441. (c) D'Oria, E.; Karamertzanis, P. G.; Price, S. L. *Cryst. Growth Des.* **2010**, *10*, 1749. (d) Li, Z. J.; Ojala, W. H.; Grant, D. J. W. *J. Pharm. Sci.* **2001**, *90*, 1523. (e) Li, Z. J.; Zell, M. T.; Munson, E. J.; Grant, D. J. W. *J. Pharm. Sci.* **1999**, *88*, 337.

(12) (a) Collier, E. A.; Davey, R. J.; Black, S. N.; Roberts, R. J. *Acta Crystallogr.* **2006**, *A62*, 498. (b) Black, S. N.; Collier, E. A.; Davey, R. J.; Roberts, R. J. *J. Pharm. Sci.* **2007**, *96*, 1053.

(13) Staples, R. J.; Cho, E. *Z. Kristallogr.-New Cryst. Struct.* **2005**, *220*, 543.

(14) Gossner, N. *Z. Kristallogr., Kristallgeom., Kristallphys., Kristallchem.* **1934**, *89*, 417.

(15) Sheldrick, G. M. *Acta Crystallogr.* **2008**, *A64*, 112.

(16) Etter, M. C. *Acc. Chem. Res.* **1990**, *23*, 120.

(17) Macrae, C. F.; Bruno, I. J.; Chisholm, J. A.; Edgington, P. R.; McCabe, P.; Pidcock, E.; Rodriguez Monge, L.; Taylor, R.; van de Streek, J.; Wood, P. A. *J. Appl. Crystallogr.* **2008**, *41*, 466.

(18) Duddu, S. P.; Grant, D. J. W. *Pharm. Res.* **1994**, *11*, 1549.

(19) Childs, S. L.; Wood, P. A.; Rodriguez-Hornedo, N.; Sreenivas Reddy, L.; Hardcastle, K. I. *Cryst. Growth Des.* **2009**, *9*, 1869.

(20) (a) Guerrieri, P.; Rumondor, A. C. F.; Li, T.; Taylor, L. S. *AAPS PharmSciTech* **2010**, *11*, 1212. (b) Anderson, B. D.; Conradi, R. A. *J. Pharm. Sci.* **1985**, *74*, 815.